Neuron, Vol. 21, 727–739, October, 1998, Copyright ©1998 by Cell Press

SAP90 Binds and Clusters Kainate Receptors Causing Incomplete Desensitization

Elizabeth P. Garcia,*‖ Sunil Mehta,*‖
Leslie A. C. Blair,* David G. Wells,†
Jing Shang,* Teruyuki Fukushima,*
Justin R. Fallon,† Craig C. Garner,‡
and John Marshall*§
*Department of Molecular Pharmacology, Physiology, and Biotechnology
†Department of Neuroscience
Brown University
Providence, Rhode Island 02912
‡Neurobiology Research Center
University of Alabama at Birmingham
Birmingham, Alabama 35213-2185

Summary

The mechanism of kainate receptor targeting and clustering is still unresolved. Here, we demonstrate that members of the SAP90/PSD-95 family colocalize and associate with kainate receptors. SAP90 and SAP102 coimmunoprecipitate with both KA2 and GluR6, but only SAP97 coimmunoprecipitates with GluR6. Similar to NMDA receptors, GluR6 clustering is mediated by the interaction of its C-terminal amino acid sequence, ETMA, with the PDZ1 domain of SAP90. In contrast, the KA2 C-terminal region binds to, and is clustered by, the SH3 and GK domains of SAP90. Finally, we show that SAP90 coexpressed with GluR6 or GluR6/KA2 receptors alters receptor function by reducing desensitization. These studies suggest that the organization and electrophysiological properties of synaptic kainate receptors are modified by association with members of the SAP90/PSD-95 family.

Introduction

Glutamate, the major excitatory neurotransmitter in the mammalian brain, gates three types of ionotropic receptors, NMDA, AMPA, and kainate, based on their pharmacology in vivo and the properties of cloned receptor subunits (Seeburg, 1993; Hollmann and Heinemann, 1994). Molecular approaches have demonstrated that a variety of subunits can contribute to the formation of native kainate receptors. While the GluR5-GluR7, KA1, and KA2 subunits all encode kainate-binding receptors, not all combinations produce ligand-gated responses. Individual expression of GluR5, GluR6, or GluR7 subunits results in homomeric receptors that respond to glutamate or kainate with rapidly desensitizing current (Bettler et al., 1990; Egebjerg et al., 1991; Schiffer et al., 1997; Swanson et al., 1997). KA1 and KA2 are functional only when coexpressed with either GluR5, GluR6, or GluR7, suggesting that KA1 and KA2 form heteromeric complexes with GluR5–GluR7 subunits in the CNS (Wenthold et al., 1994; Schiffer et al., 1997). Although heteromers containing KA1 or KA2 also generate fast and fully desensitizing currents, in addition to glutamate and kainate, they are also sensitive to AMPA (Herb et al., 1992; Schiffer et al., 1997).

Until recently, the overlapping abilities of ligands to activate both AMPA and kainate receptors have made it difficult to study receptor subtypes in vivo. With the advent of specific kainate receptor antagonists (Clarke et al., 1997) and the 2,3-benzodiazepine AMPA receptor antagonists, it is now possible to separate native AMPA and kainate receptors (Paternain et al., 1995; Lerma, 1997). Significantly, when kainate responses were examined, differing results were obtained. While fast and fully desensitizing kainate responses were observed in dorsal root ganglia (Huettner, 1990) and embryonic hippocampal neurons (Lerma et al., 1993), incompletely desensitizing responses occurred in response to kainate and, to a lesser degree, glutamate in hippocampal cultures prepared from postnatal rats (Wilding and Huettner, 1997). Additionally, in the hippocampal mossy fiber–CA3 neuron connection, synaptic release of glutamate was found to elicit slowly desensitizing kainate receptor currents (Castillo et al., 1997; Vignes and Collingridge, 1997). The molecular mechanism underlying these differences is unknown.

Glutamate receptors are primarily localized to postsynaptic densities (PSD), which also contain signaling proteins, cytoskeletal elements, and members of the SAP90/PSD-95 family (SAPs) (Ehlers et al., 1996a; Kennedy, 1997; Pawson and Scott, 1997). SAPs, which contain three PDZ domains followed by an SH3 domain and an enzymatically inactive guanylate kinase (GK) domain (Kuhlendahl et al., 1998), have been postulated to organize the signaling matrix within PSDs via these specific domains (Kim et al., 1995; Pawson and Scott, 1997). SAP90 (also known as PSD-95) (Cho et al., 1992; Kistner et al., 1993) and other SAPs (Müller et al., 1995, 1996; Hunt et al., 1996; Kim et al., 1996) have now been shown to bind to and cluster a number of ion channels, including NMDA receptors, via an interaction between the SAP PDZ domain and a C-terminal ET/SXV sequence motif in the ion channel (Kornau et al., 1995; Kim et al., 1996; Müller et al., 1996; Niethammer et al., 1996; reviewed, Sheng, 1996).

Here, we demonstrate that members of the SAP90/PSD-95 family colocalize and associate with kainate receptors in vivo and in vitro. Moreover, coexpression of SAP90 with recombinant kainate receptor subunits decreases desensitization. These results suggest that native GluR6/KA2 receptors associated with SAP proteins exhibit slow desensitization properties.

Results

Kainate Receptors Interact Biochemically with SAP90/PSD-95 Proteins

It has been proposed that members of the SAP90/PSD-95 family of proteins cluster NMDA receptors at postsynaptic sites via direct binding to the C terminus of ion

§To whom correspondence should be addressed (e-mail: john_marshall@brown.edu).
‖These authors contributed equally to this work.

channels, thus facilitating synaptic organization (Kornau et al., 1995; Kim et al., 1996; Müller et al., 1996; Niethammer et al., 1996). Given that kainate receptors have been localized in glutamatergic synapses, we examined whether members of the SAP90/PSD-95 family could interact biochemically with the kainate receptor subtypes, KA2 and GluR6. As indicated in Figure 2A, SAP90, SAP102, and SAP97 from brain extracts coimmunoprecipitate with native GluR6 (lane 6). In contrast, KA2 clearly coimmunoprecipitates SAP90 and SAP102, but not SAP97 (lane 8). As expected, GluR1 fails to associate with any of these SAPs (Müller et al., 1996) (lane 3), while NR2A interacts with the postsynaptically localized SAPs, but not with the presynaptic SAP97 (Müller et al., 1995) (lane 4). Antibody specificity was confirmed by preabsorption of immunoprecipitating antibodies with antigen (lanes 5 and 7), and, in the absence of the primary anti-receptor antibody, SAPs are not precipitated (lane 2). These experiments demonstrate that KA2, GluR6, and SAPs are present in the same macromolecular complexes in vivo, but they do not reveal whether binding between KA2 and GluR6 and SAPs is direct.

To assess binding between KA2 or GluR6 and SAP90, HEK293 cells were cotransfected with different combinations of cDNAs encoding these proteins. Antibodies directed against GluR6 or KA2 were then used to immunoprecipitate the antigen plus any tightly associated proteins. Western blot analysis using anti-SAP90 antibodies demonstrates that SAP90 and GluR6 are coimmunoprecipitated (Figure 2B, lane 6). Similarly, SAP90 is coimmunoprecipitated with KA2 (Figure 2B, lane 9), indicating that both KA2 and GluR6 interact with SAP90. When GluR6 or KA2 is transfected individually, SAP90 is not coprecipitated, indicating that SAP90 is not endogenously expressed in the HEK293 cells (Figure 2B, lanes 4 and 7). As expected, no reaction was obtained from transfected cells when the immunoprecipitating antibody was preabsorbed with antigen (Figure 2B, lanes 5 and 8). As a control, we also determined that coexpression of SAP90 with GluR6 and KA2 did not alter SAP90 expression levels. When HEK293 cells were transfected with 0.5 μg of c-myc-SAP90 cDNA alone or in combination with either KA2 or GluR6, and the amounts of SAP90 detectable by Western blot compared, bands of indistinguishable intensity were obtained (Figure 2B, lanes 1–3), implying that similar amounts of SAP90 were expressed in all conditions.

We next wanted to determine the region of KA2 important for binding SAP proteins. As the C-terminal domain of KA2 is predicted to be cytosolic, we investigated whether this region was sufficient for binding SAP90. A recombinant histidine-tagged C-terminal fragment of KA2 (H_6KA2[c-term]; Figure 1A) was purified and bound to Ni^{+2}/NTA sepharose beads and incubated with Triton X-100 solubilized extracts of either untransfected HEK293 or SAP90-transfected HEK293 cells. H_6KA2(c-term) and any associated proteins were specifically eluted using an imidazole gradient and subjected to Western blot analysis (Figure 2C). As controls, the extracts were also incubated with either naked Ni^{+2}/NTA beads or with H_6rbSec1A prebound to Ni^{+2}/NTA beads. H_6rbSec1A (Garcia et al., 1996) was used as a control because it was produced in the same vector and thus contains the same amino acid linker between the histidine tag and the sequence of interest. We find that SAP90 coelutes with the H_6KA2(c-term) (Figure 2C, top panel, lane 6), but not with the H_6rbSec1A or naked Ni^{+2}/NTA bead controls (Figure 2C, top panel, lanes 5 and 7). Elution of untransfected HEK293 cell extracts demonstrates that there are no cross-reactive bands detected with the anti-SAP90 antiserum, thus reaffirming that SAP90 is not endogenously produced in the HEK293 cells (Figure 2C, top panel, lanes 2–4). Immunoblotting of H_6KA2(c-term) and H_6rbSec1A (Figure 2C, middle and lower panels) further suggests that similar amounts of proteins were eluted from each of the Ni^{+2}/NTA sepharose bead columns. Additionally, because Ca^{2+} may play a role in the cytoskeletal organization of macromolecular complexes (Wyszynski et al., 1997) and be involved in desensitization of glutamate receptors (Ehlers et al., 1996b), we specifically addressed whether Ca^{2+} could influence binding. Experiments, using affinity chromatography approaches, revealed that H_6KA2(c-term) interacts with

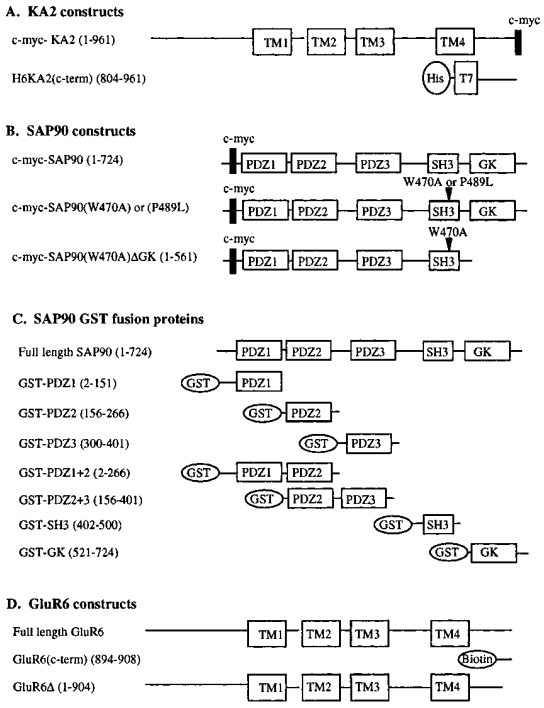

Figure 1. Schematic Representation of the DNA Constructs Used in This Study

(A) KA2 DNA constructs. The domains of c-myc-tagged KA2 are indicated, including the four transmembrane regions (TM) and the C-terminal c-myc epitope. For H_6KA2(c-term), the histidine tag (His), location of the T7 epitope (T7), and the portion of KA2 included are indicated. KA2 amino acid residues included in each construct are indicated in parentheses.

(B) SAP90 constructs used in eukaryotic expression vectors. Shown are diagramatic representations of the domains, the location of the c-myc epitope, the location of the SH3 mutations (W470A or P489L), and the deletion of the GK domain. The amino acid residues of SAP90 are indicated in parentheses.

(C) Schematic representations of SAP90-GST fusion proteins show the regions of SAP90 that were expressed as GST-fusion proteins.

(D) GluR6 DNA constructs. Shown are the full-length GluR6, GluR6Δ (four C-terminal amino acids deleted), and GluR6(c-term) (includes the 15 C-terminal amino acids).

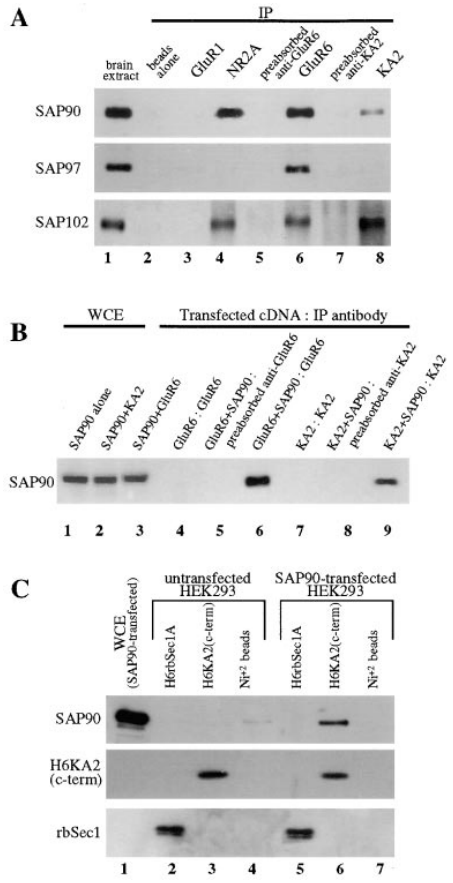

Figure 2. Members of the SAP90/PSD-95 Family Bind to Kainate Receptors

(A) KA2 and GluR6 subunits associate with SAP proteins in vivo. Antibodies directed against GluR1, NR2A, GluR6, or KA2 were used to immunoprecipitate receptors from rat brain extracts. Immunoprecipitated proteins were separated by SDS-PAGE, transferred to nitrocellulose, and immunoblotted with anti-SAP90, SAP97, or SAP102 antibodies as indicated. Controls lanes are 5 μg crude brain extract (no immunoprecipitation), beads alone (no primary antibody), and preabsorption of primary antibodies with antigen.

(B) SAP90 protein coimmunoprecipitates with GluR6 and KA2 in transfected HEK293 cells. As indicated over each lane, cells were transfected with GluR6 or KA2 cDNA alone or in combination with SAP90 cDNA. Extracts were immunoprecipitated with anti-GluR6 or anti-KA2 antibodies and immunoblotted using anti-SAP90 antibodies. Lanes 1–3, 5 μg of whole-cell extract (WCE) of SAP90-, SAP90+KA2-, and GluR6+SAP90-transfected cells; note that coexpression of SAP90 with GluR6 and KA2 does not alter SAP90 expression levels.

(C) SAP90 binds to the C terminus of KA2. Extracts of either untransfected HEK293 cells (lanes 2–4) or SAP90-transfected HEK293 cells (lanes 5–7) were incubated with Ni^{+2}/NTA sepharose beads that had been prebound with H_6KA2(c-term), H_6rbSec1A, or no protein (Ni^{+2} beads alone) overnight and washed extensively. Bound proteins were specifically eluted, separated by SDS-PAGE, transferred to nitrocellulose, and probed with either an anti-SAP90 (top panel), or an anti-T7 antibody to detect H_6KA2(c-term) and H_6rbSec1A (middle and lower panels). Lane 1, 10 μg of whole-cell extract (WCE) of SAP90-transfected cells.

SAP90 in a Ca^{2+}-independent manner (data not shown). The above results show that KA2-SAP90 binding is mediated via its cytosolic C terminus.

KA2 and GluR6 Directly Bind to Distinct SAP90 Domains

While the C terminus of GluR6 (ETMA) shows similarity to the ET/SXV consensus motif utilized by other ion channels to bind SAP90, the C terminus of KA2 is completely unrelated (TEHE). To determine how KA2 receptors bind SAP90, we employed a combination of in vitro binding assays. We constructed GST fusion proteins where each domain of SAP90 was either fused individually to GST or in combination with one adjacent domain (Figure 1C). Equal amounts of purified GST-SAP90 fusion proteins prebound to glutathione sepharose beads were incubated with purified H_6KA2(c-term). After extensive washing, beads were treated with 10 mM glutathione to release the GST-SAP90 fusion proteins and any associated H_6KA2(c-term). The eluates were separated by SDS-PAGE, transferred to nitrocellulose, and probed for the presence of H_6KA2(c-term) using a monoclonal antibody directed against a T7 epitope, located in the linker region between the histidine tag and the beginning of the C-terminal sequence of KA2 (Figure 1A).

As shown in Figure 3A, H_6KA2(c-term) binds to both the SH3 and GK domains of the GST-SAP90 fusion proteins, but not to any of the GST-PDZ domains or to GST alone. Because the C terminus of KA2 contains two proline-rich sequences, it is likely that conserved residues within the SAP90 SH3 domain mediate this interaction. To confirm the specificity of the SH3–KA2 interaction, we introduced a single amino acid substitution within the SH3 domain, tryptophan-470 to alanine (W470A), shown to disrupt the ability of SH3 domains to bind proline-rich regions (Erpel et al., 1995). H_6KA2(c-term) was incubated with GST, GST-SH3, or GST-SH3W470A prebound to glutathione sepharose beads. Bound proteins were eluted and analyzed as in Figure 3A. We find that H_6KA2(c-term) binds to GST-SH3 but not to GST and only minimally to GST-SH3W470A (Figure 3B, left panel), suggesting that the SH3–KA2 interaction is mediated by proline-rich sequences in the KA2 C-terminal region. To determine whether H_6KA2(c-term) would bind to other SH3 domains, we assessed the ability of H_6KA2(c-term) to bind GST-Grb2 (McPherson et al., 1996), an SH3-SH2-SH3 adaptor protein fused to GST. As shown in Figure 3B (right panel), H_6KA2(c-term) binds GST-SH3, but not glutathione sepharose beads GST or GST-Grb2, suggesting specificity for a subset of SH3 domains. Control experiments were carried out to demonstrate that GST-SH3 and GST-GK bound specifically to H_6KA2(c-term) and not to other histidine-tagged recombinant proteins (Figure 3C). GST-SH3 and GST-GK prebound to glutathione beads were incubated with equal amounts of H_6KA2(c-term), H_6rbSec1A, thioredoxin-α-bungarotoxinT68-H_6 (TrxαT68-H_6), or H_6α-bungarotoxin (H_6αBgTx) and processed as in Figure 3A. To detect the presence of bound histidine-tagged recombinant proteins, Western blots were carried out using anti-penta-histidine antibody (Qiagen). Again, while H_6KA2(c-term) coelutes with GST-SH3 and GST-GK, none of the other hisitidine-tagged proteins were bound, indicating that the SH3–KA2 and GK–KA2 interactions are specific. We also show that GST-SH3 and GST-GK do not bind to full-length GluR6 or the C-terminal fragment of GluR6 (Figure 4, see below).

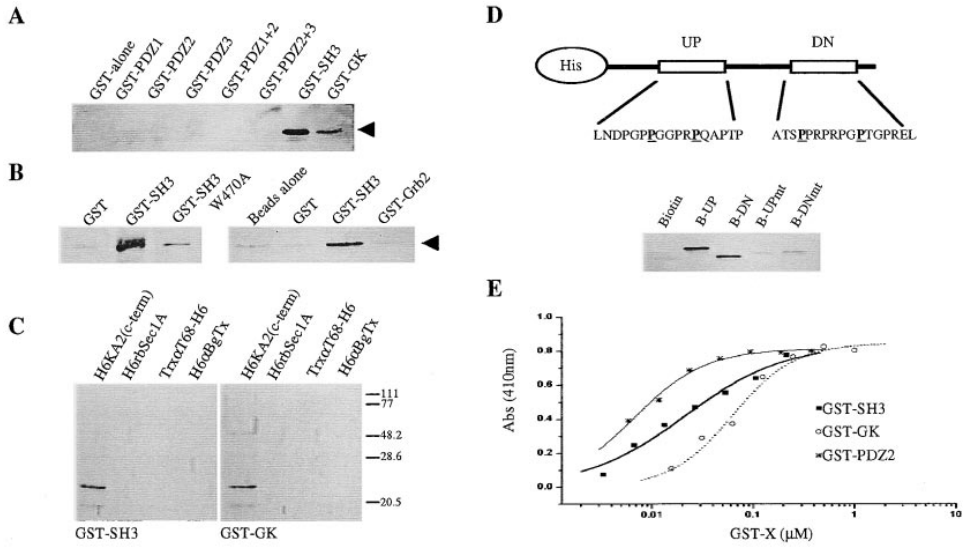

Figure 3. KA2 Binding to SAP90 Is Mediated by the SH3 and GK Domains

(A) H_6KA2(c-term) binds GST fusion proteins containing the SH3 and GK domains of SAP90. Twenty micrograms of H_6KA2(c-term) was incubated with 10 μg of each of the GST-SAP90 fusion proteins or GST alone prebound to 20 μl glutathione sepharose beads as indicated above the panel. Following extensive washes, bound proteins were eluted with 10 mM glutathione, separated by SDS-PAGE, and transferred to nitrocellulose. H_6KA2(c-term) was visualized by immunoblotting with antibodies directed against the T7 epitope. Arrowheads denote the position of H_6KA2(c-term).

(B) H_6KA2(c-term) was incubated with each of the fusion proteins as indicated above the panels and processed as described in (A). Arrowheads denote the position of H_6KA2(c-term).

(C) SAP90 fusion proteins GST-SH3 and GST-GK bind specifically to H_6KA2(c-term) and not to other hisitidine-tagged recombinant proteins. Histidine-tagged proteins were detected using anti-penta-histidine antibody (Qiagen) and visualized by chemiluminesence. Molecular weights (kDa) are indicated.

(D) The SAP90 SH3 domain binds to both proline-rich sequences present in H_6KA2(c-term). The relative location and sequence of the C-terminal (UP) and N-terminal (DN) proline-rich sequences are drawn schematically. Proline residues that are bolded and underlined were mutated to alanine residues to form the UP and DN mutants (B-UPmt and B-DNmt, respectively). Each of these regions fused to biotin, or biotin alone, was incubated with the GST-SH3 prebound to glutathione beads. Bound proteins were eluted and processed as in (A). Biotinylated proteins were detected using anti-biotin antibody (Sigma).

(E) Dose response curves of SAP90 SH3 and GK domains binding to the C terminus of KA2. H_6KA2(c-term) was bound and incubated with the SAP90 fusion proteins GST-SH3 or GST-GK. As an internal control, the dose response curve of GST-PDZ2 of SAP90 binding to Bio-NR2B-9 (Müller et al., 1996) was also determined. The data were fit with the Hill equation ($Abs = Abs_{max}/1+[EC50/[X]]^n$; Abs = absorbance at 410 nm) using a nonlinear least-squares algorithm.

The KA2 C terminus has two proline-rich domains that contain the core amino acid sequence of some class II peptides, PXXPR (Weng et al., 1995). To determine which of these domains is responsible for SH3 binding, we individually subcloned each of the proline-rich domains (UP and DN) shown schematically in Figure 3D into Pinpoint Xa-3 (Promega) producing biotinylated fusion proteins, B-UP and B-DN, and tested their ability to bind GST-SH3. While GST-SH3 did not bind to the biotin-labeled fusion partner (Figure 3D, Biotin lane), GST-SH3 bound to both the UP and DN proline-rich sequences (B-UP and B-DN lanes). To address the specificity of the interaction, we mutated two proline residues to alanine in each proline-rich domain (Figure 3D, indicated by boldface, underscored P) to eliminate PXXP motifs, the minimum sequence required for binding to SH3 domains (Mayer and Eck, 1995). As shown, GST-SH3 no longer binds to either B-UPmt or B-DNmt, consistent with the hypothesis that a PXXP motif is required for SH3 binding.

We also performed binding assays to determine the affinities between the C-terminal domain of KA2 and the SH3 and GK domains of SAP90. As indicated in Figure 3E, the KA2 C terminus binds the SH3 domain of SAP90 with an apparent K_d of 20 nM and the GK domain with a K_d of 63 nM. As an internal control, the binding affinity of the NMDA receptor NR2B subunit C terminus to the SAP90 PDZ2 domain was determined to be 7 nM, similar to the values previously reported for NR2B interactions with SAP102 and SAP90 PDZ2 domains (6 nM; Müller et al., 1996).

To determine the region of SAP90 that interacts with GluR6, equal amounts of each of the GST-SAP90 fusion proteins were prebound to glutathione-sepharose beads. Detergent-solubilized extracts prepared from GluR6-transfected HEK293 cells were incubated with each of the GST-SAP90 fusion proteins bound to beads. After extensive washing, the fusion proteins plus any associated proteins were specifically eluted from the beads using glutathione. Aliquots were immunoblotted for the presence of GluR6. As shown in Figure 4A, GluR6 binds strongly to the PDZ1 and PDZ1+2 domains of SAP90 fused to GST, but only minimally to PDZ2 or PDZ2+3 domains. Importantly, identical results are obtained when binding of a C-terminal fragment of GluR6 (GluR6[c-term]; Figure 1D) is tested against the PDZ fusion proteins

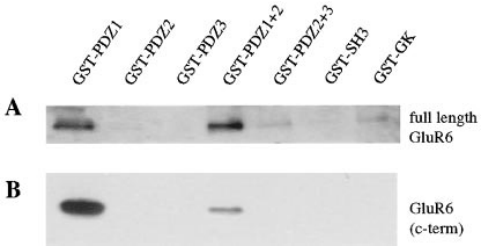

Figure 4. GluR6 Binding Is Mediated by the SAP90 PDZ1 Domain

(A) GluR6 binds PDZ1. Extracts prepared from GluR6-transfected HEK293 cells were incubated with the various GST-SAP90 fusion proteins prebound to glutathione-sepharose beads. GST-SAP90 fusion proteins and any associated proteins were specifically eluted and separated by SDS-PAGE, transferred to nitrocellulose, and immunoblotted with anti-GluR6 antibodies.

(B) PDZ1 specifically binds the C-terminal sequence of GluR6. A recombinant biotinylated 15 amino acid peptide corresponding to the GluR6 C terminus was incubated in solution with GST-SAP90 fusion proteins prebound to glutathione-sepharose beads and then processed as in (A).

(Figure 4B), demonstrating that SAP90 binds GluR6 through interaction of its PDZ1 domain with C-terminal residues on the receptor.

Kainate Receptors Are Clustered by Members of the SAP90/PSD-95 Family

As a further measure of the ability of kainate receptors to interact with SAP90 family members, we used confocal microscopy to assess the ability of SAP90 to change the receptor distribution. A c-myc-tagged SAP90 cDNA was prepared (Figure 1B) and transfected into COS-1 cells. SAP90 distribution was then detected by anti-c-myc immunolabeling and indirect immunofluorescence.

Kainate receptor subtypes were cotransfected with the c-myc-SAP90 into COS-1 cells (Figure 5A). For controls, the SAP90, KA2, and GluR6 constructs were transfected individually, producing in each case diffuse staining (Figure 5A, a–c). However, when cells were cotransfected with c-myc-SAP90 and either KA2, GluR6, or KA1, clustering clearly occurs (Figure 5A, d–g). To ensure that SAP90-induced clustering was not an artifact caused by the presence of the c-myc epitope on SAP90, we performed additional experiments, cotransfecting native SAP90 with c-myc-tagged KA2. Clustering was evident when both c-myc-KA2 and SAP90 were present, but in the absence of SAP90, c-myc-KA2 exhibited a diffuse staining pattern (data not shown). Additional controls were carried out demonstrating that coexpression of SAP90 with GluR6 and KA2 did not alter SAP90 expression levels (Figure 2B, lanes 1–3).

To determine whether kainate receptors and SAP90 are present in the same clusters, double labeling was performed. As shown in Figure 5A (d and e), both KA2 and SAP90, and GluR6 and SAP90 clusters colocalize. To demonstrate surface receptor clustering, labeling was also done using an anti-GluR6 antibody that recognizes an extracellular epitope (Huntley et al., 1993) (Figures 5A, e, f, and j and 5B, h). Specifically, receptor- and SAP90-cotransfected cells were fixed without permeabilization, labeled to identify plasmalemmal GluR6 receptors, and then either directly processed for immunofluorescence (Figure 5A, f and j) or subsequently permeabilized and incubated with antibodies against intracellular targets (SAP90, Figure 5A, e; or the C terminus of KA2, Figure 5B, h). To further ensure that the GluR6 clusters were plasmalemmal, we tested whether fixation could allow antibody access to the cytoplasm; when standardly fixed cells were not permeabilized, no SAP90 labeling is obtained even though surface clusters of GluR6 are still observed (Figure 5A, f).

Interestingly, COS-1 cells triply transfected with SAP90, GluR6, and either KA2 or KA1 (Figure 5A, h–j) showed larger, brighter clusters than in cells that had been cotransfected with SAP90 and a single kainate receptor subtype. Typically, approximately 90% of the SAP90-cotransfected cells showed detectable clustering. When cluster diameters were measured, it was found that expression of SAP90 with both receptor subunits dramatically increased the cluster size (mean $\pm$ SEM, n = 30 for each group; 9.4 $\pm$ 0.9 μm^2 for GluR6+KA2+SAP90 compared to 2.6 $\pm$ 0.3 μm^2 for KA2+SAP90 and 3.8 $\pm$ 0.4 μm^2 for GluR6+SAP90). The mechanism underlying this difference remains to determined. However, because KA2 and GluR6 bind distinct SAP90 domains, clustering effects may be additive or even synergistic when both subunits are coexpressed with the SAP90 protein. Finally, to examine whether other SAPs were also effective, we tested coexpression with chapsyn-110, a SAP protein known to cluster heterologously expressed Kv1.4 channels and NMDA receptors (Kim et al., 1996, Niethammer et al., 1996) and find that it efficiently clusters kainate receptors as well (Figure 5A, k and l).

The SH3 and GK Domains of SAP90 Are Required for KA2 Clustering

The potential roles of the SH3 and GK domains in clustering KA2 channels were investigated separately and in tandem. Our biochemical data strongly suggest that the SH3 domain of SAP90 binds to the proline-rich sequences in the C terminus of KA2 (Figure 3D), and that the introduction of a W470A amino acid substitution abrogates binding of the SH3 domain to the C terminus of KA2 (Figure 3B). Two SAP90 cDNAs, one containing the W470A mutation and another where proline-489 was mutated to leucine (P489L), were constructed resulting in c-myc-tagged cDNA clones, SAP90(W470A) and SAP90(P489L), respectively (Figure 1B). These residues were chosen, as both residues are conserved in all currently identified SAPs, and mutation of either abolishes not only binding to proline-rich sequences, but also SH3 signaling functions (Erpel et al., 1995).

Transfection of c-myc-SAP90(W470A) or c-myc-SAP90 (P489L) individually into COS-1 cells yielded as expected a diffuse staining pattern (data not shown). Surprisingly, however, cotransfection of KA2 with either SAP90(W470A) or SAP90(P489L) still caused clustering (Figure 5B, a and b). Because these mutations failed to eliminate clustering, we proceeded to delete the GK domain, creating a SAP90 cDNA, SAP90ΔGK, that was truncated at amino acid 561. Again, the mutated SAP90 still efficiently clustered KA2 (Figure 5B, c). As compared to cells that had been transfected with c-myc-SAP90

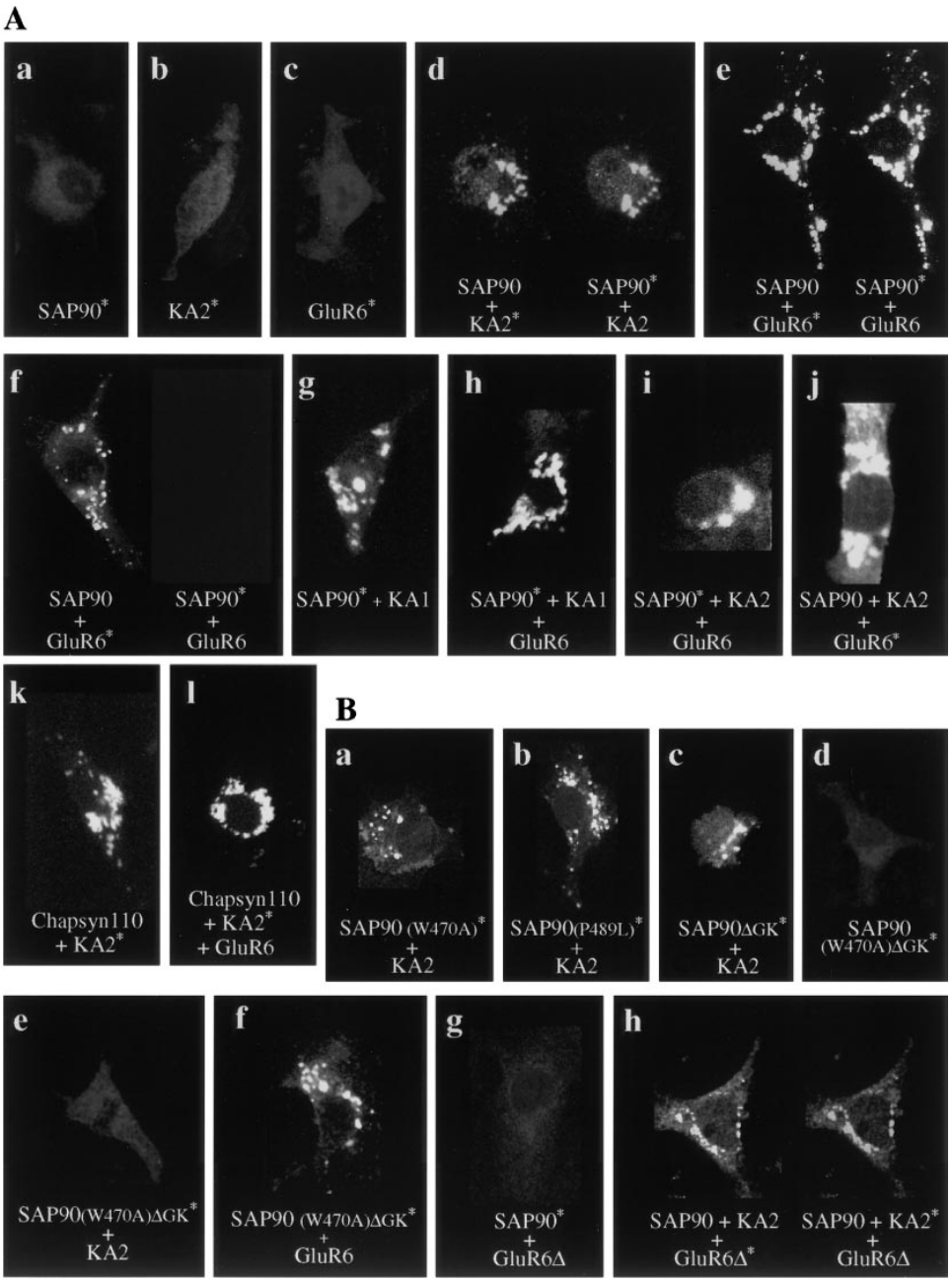

Figure 5. The SAP90/PSD-95 Family of Proteins Clusters Kainate Receptors in Transfected COS-1 Cells

(A) SAP90 clusters kainate receptors. COS-1 cells were transfected with the cDNAs listed at the bottom of each panel, and clustering was assessed by indirect immunofluorescence. Asterisks indicate the antibody target. (a–c) SAP90, KA2, or GluR6 is diffusely distributed when expressed individually. (d, e, and g) Coexpression of SAP90 with either KA2, GluR6, or KA1 results in coclustering. (f and j) In the absence of permeabilization, surface clusters of GluR6 receptors are detected, even though labeling of the intracellular SAP90 is blocked (f). (h–j) Simultaneous coexpression of SAP90+GluR6 and either KA2 or KA1 results in larger clusters. (k and l) Similarly, chapsyn-110 induces clustering of KA2 and KA2+GluR6 receptors. Labeling is described in detail in Experimental Procedures. Briefly, primary antibodies were anti-KA2, anti-GluR6 (C-terminal epitope, [A, c]), anti-GluR6 (extracellular epitope, all other GluR6 labeling), or an anti-c-myc antibody to recognize c-myc-tagged SAP90. Secondary antibodies were FITC conjugated (A, a, b, d–i and B, a–h) or Cy3 conjugated (A, c–f, j and B, h). Labeling was visualized by confocal microscopy. For cells labeled with anti-extracellular domain GluR6 antibody, labeling was performed in the absence of permeabilization (A, f and j) or before the permeabilization required for subsequent labeling of intracellular epitopes (A, e and B, h).

(B) Identification of domains necessary for SAP-mediated kainate receptor clustering. COS-1 cells were transfected with the cDNAs listed at the bottom of each panel; the c-myc-tagged SAP90 mutants are shown in Figure 1B; for GluR6Δ, the last four amino acids were deleted (Figure 1D). (a–c) When SAP90 cDNAs, altered to remove amino acids essential for SH3 or GK function, are coexpressed with KA2, clustering still results. (d–f) Expression of a SAP90 cDNA, altered to remove both SH3- and GK-binding functions. (d) No self-clustering is observed when this SAP90 construct is expressed alone. (e) Coexpressed with KA2, clustering is abolished. (f) In contrast, when coexpressed with GluR6, clustering occurs. (g and h) GluR6 altered to delete the four C-terminal amino acids. (g) Coexpressed with native SAP90, GluR6 clustering is abolished. (h) However, coexpression with native SAP90 and KA2 restores the ability to cluster, suggesting that heteromeric receptors are being anchored via SAP90.

and KA2 (Figure 5A, d), there was no qualitative difference in the clusters.

To examine the possibility that each domain, either SH3 or GK, could separately mediate KA2 clustering, we introduced both the SH3 mutation W470A and the GK deletion into a single construct, SAP90(W470A)ΔGK (Figure 1B), which, when expressed alone, shows a diffuse distribution (Figure 5B, d). Significantly, staining remains diffuse upon cotransfection with KA2 (Figure 5B, e), indicating that both domains independently confer the ability to cluster KA2. Importantly, though, the double mutation has not otherwise impaired the SAP90 protein; clustering is still evident when SAP90(W470A) ΔGK is cotransfected with GluR6 (Figure 5B, f). These data support the concept that KA2 and GluR6 clustering are mediated via distinct SAP90 domains.

As shown in Figure 4, the C terminus of GluR6 interacts biochemically with the SAP90 PDZ1 domain. Moreover, although its C-terminal sequence (ETMA) is not identical to the sequences known to mediate SAP binding to other ion channels (reviewed, Sheng, 1996), it does strongly resemble them. To determine whether SAP90 induces GluR6 clustering via this sequence, we constructed a GluR6Δ cDNA (Figure 1D) to encode a truncated receptor missing its four C-terminal amino acids, and then cotransfected cells with SAP90 and either GluR6Δ or GluR6 cDNA. The results imply that SAP90 clusters GluR6 receptors via this "atypical" C terminus; although clusters are evident in the GluR6+SAP90 cotransfected cells (Figure 5A, e), no clustering was observed when GluR6Δ and SAP90 were cotransfected (Figure 5B, g). Moreover, as would be expected if only KA2 was able to bind SAP90, coexpression of GluR6Δ with KA2+SAP90 results in the formation of clusters similar to those observed with KA2+SAP90 (Figure 5B, h). Interestingly, the clusters in the triply transfected cells colabel with both anti-GluR6 (extracellular domain) and anti-KA2 antibodies (Figure 5B, h), suggesting that heteromeric receptors may be present and confirming surface clustering.

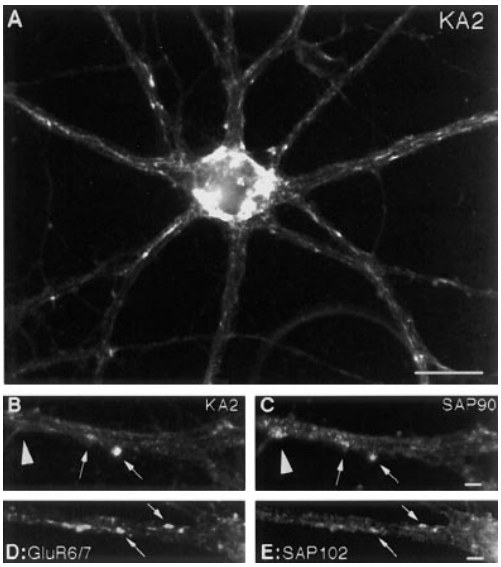

Figure 6. Kainate Receptors Colocalize with SAP90 and SAP102 in Hippocampal Neuron Cultures

Primary cultures of 28-day-old hippocampal neurons were labeled with anti-KA2 (A) or double labeled with anti-KA2 (B) and anti-SAP90 (C), or anti-GluR6/7 (D) and anti-SAP102 (E) antibodies. Arrows indicate sites of KA2+SAP90 and GluR6/7+SAP102 colocalization in the dendrites. Additionally, SAP clusters not containing KA2 can also be observed (B and C; arrowheads). Scale bars, 20 μm (A) and 5 μm (B–E).

Kainate Receptors Colocalize with SAPs in Hippocampal Neuron Cultures

We were particularly interested in establishing in vivo association or role of SAPs with kainate receptors. We therefore performed immunocytochemical colocalization studies on cultured hippocampal neurons, as well as the coimmunoprecipitation experiments on rat brain extracts (Figure 2A). Low-density hippocampal cultures were prepared as previously described (Goslin and Banker, 1991). By 20 days in culture, hippocampal neurons have well-defined postsynaptic densities similar to those identified in mammalian brain, and the synaptic organization should mimic what is observed in vivo (Bartlett and Banker, 1984; Craig et al., 1993). When we examine the processes of 28-day-old hippocampal neurons, clusters of KA2 receptors (Figure 6A) and SAP90 are readily evident. To determine whether KA2 and SAP90 are present in the same clusters, we performed double labeling experiments. As indicated in Figures 6B and 6C (see arrows), KA2 and SAP90 clearly colocalize in neuronal processes. Moreover, in regions where KA2 clusters are present, SAP90 also colocalizes. However, as would be expected from the ability of SAP90 to cluster other receptor subtypes, SAP90 clusters not containing KA2 channels are also evident (Figures 6B and 6C; arrowheads). Similar findings are obtained when examining the localization of GluR6/7 and SAP102 (Figures 6D and 6E). Taken in conjunction with the ability of SAP90/SAP102 to coimmunoprecipitate with native GluR6 and KA2 receptors (Figure 2A), these data strongly imply that SAP proteins cluster kainate receptors in vivo.

SAP90 Causes Incomplete Desensitization of Kainate Receptors

Finally, we wished to determine whether coexpression of kainate receptors with SAP90 could alter receptor function. We applied standard electrophysiological approaches and rapid glutamate application. Because KA2 expressed alone does not form functional receptor channels (Herb et al., 1992), control cells were transfected with either GluR6 alone or GluR6+KA2. Consistent with previous reports, we found that expression of GluR6 or GluR6 with KA2 generates glutamate-induced currents that show rapid activation and rapid and complete desensitization (Figure 7B; n = 32 of 32 cells; Herb et al., 1992). In contrast, we found that cells coexpressing GluR6, KA2, and SAP90, the conditions that produced the most dramatic clustering (Figure 5A, i and j), revealed rapid responses with incomplete desensitization (n = 22 of 25 cells [88%]; 2–5 applications of 100 μM glutamate/cell). Figures 7A and 7C are representative; glutamate induces an initial peak that rapidly but only

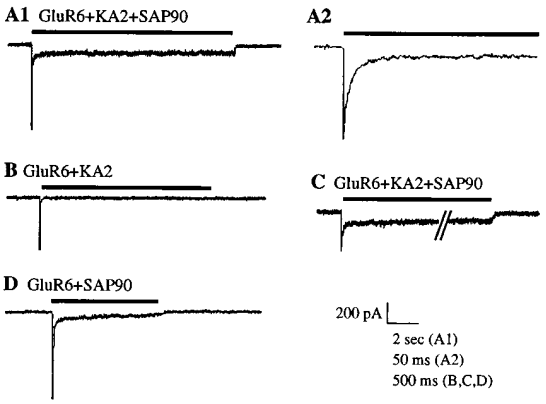

Figure 7. Coexpression of Kainate Receptors with SAP90 Strongly Reduces Desensitization

(A) In cells coexpressing GluR6, KA2, and SAP90, glutamate induces incompletely desensitizing responses. A1, extended glutamate application reveals a nondesensitizing component. A2, the same record on an expanded time scale shows the initial peak. For (A)–(D), bar indicates glutamate (100 μM) application; cells (HEK293, except COS-1 in [C]) were transiently cotransfected with cDNAs encoding SAP90, GluR6, and/or KA2 plus to enable identification of transfected cells, GFP.

(B) In the absence of SAP90, responses fully and rapidly desensitize.

(C) In COS-1 cells coexpressing GluR6, KA2, and SAP90, glutamate responses (20 s application; middle section indicated by slash) only partially desensitize.

(D) Although the plateau component is typically smaller than when coexpressing SAP90 with both receptor subunits, cells cotransfected with SAP90 and GluR6 cDNAs can also exhibit incomplete desensitization.

partially desensitizes to a steady-state level that is approximately one-third of the initial peak current (0.39 ± 0.05; mean ± SEM).

Coexpression of GluR6 and SAP90 was also tested. Because SAP90 also strongly clusters homomeric GluR6 receptors (Figure 5A, e and f), even if not as dramatically, we anticipated results similar to the SAP90/GluR6/KA2 cotransfectants. Surprisingly, however, responses in GluR6/SAP90-expressing cells were intermediate between those in cells lacking SAP90 and those in cells expressing both receptor subunits with SAP90. For instance, fewer cells exhibit detectable steady-state components (n = 9 of 17 cells [53%]; Figure 7D), and, in cells demonstrating nondesensitizing components, the plateaus were a significantly smaller fraction of the peak current (0.11 ± 0.03).

When we examined the kinetics of the glutamate (100 μM)-activated currents, we found that the plateau is, effectively, at steady-state, declining only minimally during extended exposure to glutamate (5–30 s; see Figures 7A, 7C, and 7D). Moreover, inclusion of KA2 did not appear to affect this slight decline (τ =10.3 ± 3.6 s [mean ± SEM] for GluR6/SAP90 cotransfectants; τ = 13.9 ± 2.8 s for GluR6/KA2/SAP90). We further found that the rapid decline of the initial peak response did not alter detectably with the presence of SAP90; decline rates with time constants of 20.1 ± 1.2 ms, 22.1 ± 0.8 ms, and 22.6 ± 0.9 ms were obtained in cells transfected with, respectively, GluR6/SAP90, GluR6/KA2/SAP90, and either GluR6/KA2 or GluR6 alone. Together, these results suggest that SAP90-dependent clustering has no effect on rapid desensitization kinetics but induces the ability of cells to make long-lasting glutamate responses by inducing the presence of a nondesensitizing component.

Discussion

In this study we show that SAP90 binds to and clusters members of the kainate subgroup of ionotropic glutamate receptors, causing a change in their electrophysiological properties. Previously, SAPs have been shown to bind ion channels via an interaction between a PDZ domain and a C-terminal ES/TXV sequence. This paper demonstrates that clustering of GluR6 channels is mediated by binding of the SAP90 PDZ1 domain to the four C-terminal amino acids of GluR6, whereas SAP90's SH3 and GK domains specifically bind to and promote KA2 clustering.

KA2 utilizes its C-terminal region to bind the SAP90 GK and SH3 domains. SH3 binding has been predicted to be mediated by proline-rich sequences (Mayer and Eck, 1995). Because KA2 contains two C-terminal proline-rich domains, we anticipated the possibility of binding to the SAP90 SH3 domain. KA2 has proline spacings and C-terminal arginine residues similar to class II proline motifs (PPLPR) found in p68 and Shb (Weng et al., 1995). Although Grb2 also binds class II–like proline motifs, we find it does not bind KA2 (Figure 3B). This is not surprising, as Grb2 preferentially binds those ligands containing an arginine two residues C-terminal to the XPPXP motif (Sastry et al., 1995) that are absent in KA2. Also, in addition to the consensus motif, flanking residues contribute to specificity and binding affinity (Feng et al., 1995). The SAP90 SH3–KA2 interaction appears to be relatively strong, showing an apparent K_d of 20 nM. Previously reported SH3 binding affinities vary widely (1 nM up to tens of μM) and depend on the particular SH3 domain–target protein interaction (Feng et al., 1995; Lee et al., 1995; Sastry et al., 1995; Matoskova et al., 1996; Bunnel et al., 1997). KA1, which is 70% identical to KA2 at the amino acid level, may bind SAP90 in a similar way. Like KA2, it contains a PXXP, the minimal sequence required for SH3 binding (Mayer and Eck, 1995).

We unexpectedly found that KA2 also binds GK at a unique to-be-determined site. Although GKAP (Kim et al., 1997; Naisbitt et al., 1997), a novel protein of unknown function, also binds the GK domain of SAP90, it requires a 14 amino acid repeat that is absent from the C terminus of KA2 and suggests that KA2 binds GK at a unique site. Interestingly, the interactions with GK and SH3 appear to function independently. Clustering is abolished when both domains are simultaneously mutated or deleted; however, clustering still occurs if either domain is altered individually.

GluR6 binds to the PDZ1 domain of SAP90. Its four C-terminal amino acids (ETMA) are critical: deletion abrogates the ability to bind to and be clustered by SAP90. Although structural interactions of glutamate receptor sequences with PDZ1 have yet to be determined, the crystal structure of the PDZ3 domain shows that the C-terminal valine of a four amino acid consensus sequence fills a prominent hydrophobic pocket on PDZ3 (Doyle et al., 1996). Binding studies also suggest that a

hydrophobic C-terminal residue is required for PDZ–channel interactions (reviewed, Sheng, 1996). For NR2 NMDA receptors and Shaker potassium channels, the terminal residue is valine; for inward rectifying potassium channels, this residue is isoleucine. We show here that for GluR6 the C-terminal residue is alanine. This result would also suggest that GluR5, which has a similar C-terminal sequence (ETVA), may be bound and clustered via the SAP90 PDZ1 domain.

As previously demonstrated for NR2 NMDA receptors and several types of potassium channels (Kim and Sheng, 1996; Kim et al., 1996, Müller et al., 1996), we now show that kainate receptors bind to multiple members of the SAP90/PSD-95 family in vivo. GluR6 and KA2 coprecipitate with both SAP90 and SAP102. GluR6 also coprecipitates with SAP97, while KA2 does not, indicating that there is specificity among the interactions between SAPs and glutamate receptor channels. Furthermore, because SAP97 is expressed presynaptically in mammalian brain (Müller et al., 1995), its differential association with GluR6 and KA2 could potentially contribute to targeting mechanisms, helping to segregate each subunit to different parts of the neuron. Studies utilizing hippocampal neurons in culture have demonstrated that during synaptogenesis, SAP90 clusters in putative postsynaptic sites prior to NMDA receptors (Rao et al., 1998).

The presence of multiple binding motifs in SAP proteins suggests that SAPs may function to organize receptors into macromolecular signaling complexes at synaptic junctions. In addition to localizing KA2 to PSDs, the SH3 and GK domains may participate in signaling pathways that regulate PSD formation. While SH3 domains are implicated in many regulatory cascades (Pawson and Scott, 1997), the role of GK is less understood. It is possible that other proteins, such as GKAP (Kim et al., 1997), may associate with these domains in vivo and regulate the assembly or function of kainate receptors. Studies in *D. melanogaster* suggest that the GK domain plays an important role in synapse formation. Flies expressing dlgv59, a SAP90 homolog with most of the GK domain deleted (Woods and Bryant, 1991), have poorly developed neuromuscular junctions (Lahey et al., 1994). In addition to binding ion channels, PDZ domains interact with a number of potential regulatory proteins. SynGAP binds SAP90–NMDA receptor complexes in vivo and stimulates Ras GTPase activity (Kim et al., 1998), while another novel protein, CRIPT, is implicated in tethering SAP90 to cytoskeletal tubulin (Niethammer et al., 1998). Moreover, phosphorylation of Kir 2.3 by PKA modulates its ability to bind to SAP90 (Cohen et al., 1996). Both GluR5 and GluR6 contain C-terminal consensus PKA sites, and GluR6 can be phosphorylated by PKA, resulting in increased activity (Raymond et al., 1993; Wang et al., 1993). InaD, a cytoplasmic protein of five PDZ domains, has been shown utilize these domains to regulate Ca^{+2} channels and recruit signaling components (e.g., PKC) into the phototransduction cascade (Shieh and Zhu, 1996; Tsunoda et al., 1997). SAP90 may function in a similar fashion. In addition, recent work on spinal neurons suggests that glycine receptor clustering is dependent upon receptor activity (Kirsch and Betz, 1998). Similarly, deregulation of nNOS (neuronal nitric oxide synthase), which binds SAP90 (Brenman et al., 1996), causes glutamate receptor overactivity and neuronal damage (Dawson et al., 1992).

We were particularly interested in establishing whether SAP-induced clustering would modify kainate receptor function. Cloned subunits typically display rapidly desensitizing glutamate responses (reviewed, Hollmann and Heinemann, 1994). Previously, in the CNS, fast desensitizing kainate receptors had been identified in embryonic hippocampal neurons likely to be composed of homomeric GluR6 subunits (Lerma et al., 1993; Paternain et al., 1995). However, kainate receptors exhibiting incomplete desensitization were recently discovered in hippocampal cultures prepared from postnatal rats (Wilding and Huettner, 1997) and at the hippocampal mossy fiber–CA3 neuron synapse where they have been shown to exhibit slow inward current responses (Castillo et al., 1997; Vignes and Collingridge, 1997). In contrast to other hippocampal fields, LTP in this region seems to be independent of NMDA receptors (Harris and Cotman, 1986) and is likely to involve KA2, KA1, and GluR6, all of which are highly expressed in CA3 pyramidal neurons (Herb et al., 1992). We find that coexpression of both KA2 and GluR6 with SAP90 produces a larger nondesensitizing component than observed in cells expressing SAP90 with homomeric GluR6 receptors. In addition, nearly all cells coexpressing KA2-GluR6-SAP90 have a nondesensitizing phase, while only half of the GluR6-SAP90 cells contain detectable plateaus.

The finding that SAPs can bind to and alter desensitization of kainate receptors lead us to speculate that the slow desensitization properties of the native receptors described above could be due to GluR6/KA2 or GluR6/KA1 receptors in association with SAP proteins. Reduced kainate receptor desensitization contrasts sharply with the rapid desensitization of AMPA receptors, which, in many cases, may curtail postsynaptic responses despite the continued presence of glutamate (Jones and Westbrook, 1996; Otis et al., 1996). In the hippocampal mossy fiber pathway, AMPA responses dominate during low-frequency stimulation. Recent work utilizing knockout mice has demonstrated that hippocampal GluR6-containing receptors are important not only for excitatory neurotransmission, but also for kainate-induced excitotoxicity and epileptic seizures (Mulle et al., 1998). By increasing synaptic glutamate concentration during high-frequency stimulation, the kainate receptors could remain relatively active, while AMPA receptors became desensitized (Jones and Westbrook, 1996; Zorumski et al., 1996). Such a mechanism would explain why high-frequency stimulation strongly enhances kainate receptor currents (Castillo et al., 1997; Vignes and Collingridge, 1997), and it suggests that reduced kainate receptor desensitization might be significant during high-frequency stimulation, insuring high-fidelity synaptic transmission. Our results demonstrate that direct interactions between kainate receptor subtypes and SAP90 both cluster the receptors and dramatically reduce desensitization, providing potential explanations for some of the variety of glutamate responses observed in the mammalian brain.

Experimental Procedures

Mammalian DNA Expression Vectors

SAP90 and chapsyn-110 cDNAs were kindly provided by Dr. M. Sheng. The cDNAs encoding GluR5, GluR6(R), KA1, and KA2 (gifts

of Dr. J. Boulter and Dr. S. Heinemann) were subcloned into the pcDNA3 expression vector (Invitrogen). The cDNA encoding SAP97 (Müller et al., 1995) was subcloned into a pCMV neo expression vector. To insert a c-myc epitope into SAP90, a unique KpnI site was introduced by site-directed mutagenesis using QuikChange (Stratagene). A cassette containing the c-myc epitope (EQKLI SEEDL) was subcloned into this site. Mutations W470A and P489L were inserted into the c-myc-SAP90 cDNA construct by site-directed mutagenesis as described above. To delete the GK domain, c-myc-SAP90 was digested with BamHI and BglII to completion, resulting in the removal of a fragment containing the majority of the GK domain, and religated forming c-myc-SAP90ΔGK. To construct c-myc-SAP90(W470A)ΔGK, the GK domain was deleted from c-myc-SAP90(W470A) as described. GluR6(Q) was constructed from GluR6(R) by PCR mutagenesis. The c-myc epitope was inserted into the KA2 cDNA sequence at the 3′ end of the nucleotide coding sequence. GluR6Δ was generated by PCR amplification of the entire coding region of GluR6, using a mutated 3′ primer that introduced a stop codon resulting in the deletion of the C-terminal four amino acids.

Cell Culture and Transfection

Human embryonic kidney cells (HEK293) and COS-1 cells were purchased from ATCC (Rockville, MD). HEK293 and COS-1 cells, grown in DMEM supplemented with 10% fetal calf serum (37°C, 5% CO2) were transiently cotransfected with GluR6, KA2, and/or SAP90 cDNAs in the ratio 1:1:1. For affinity chromatography and immunoprecipitation experiments, cells grown in 75 mm^2 flasks were transfected at 40%–60% confluence using Lipofectamine according to manufacturers' recommendations (GIBCO BRL). For immunocytochemistry, cells were plated onto glass coverslips that had been precoated with poly-D-lysine (1 mg/ml) and transfected at low density (20%–30% confluency) using Lipofectamine. As measured by the ability to detect anti-GluR6, -KA2, or -SAP90 immunofluorescence, transfection efficiency was 50%–70%. Cluster sizes were estimated by calculating the circular area. For electrophysiological recording, the cells were cotransfected by calcium phosphate precipitation (Chen and Okayama, 1987) with GluR6, KA2, and/or SAP90 cDNAs (ratio 1:2:5), plus 2 μg of jellyfish green fluorescence protein (GFP; pGreenlantern, GIBCO BRL) cDNA to facilitate identification of transfected cells, as previously described (Marshall et al., 1995).

Low-density hippocampal neuron cultures were prepared as previously described (Goslin and Banker, 1991). Briefly, hippocampi were removed from E18 rat embryos and incubated in 0.1% trypsin for 15 min at 37°C. Cells were dissociated mechanically and plated onto poly-L-lysine-coated glass coverslips (1 mg/ml) at a density of 22,500 cells/ml in minimal essential medium (MEM; GIBCO) supplemented with 10% horse serum. The coverslips were removed from the plating media after 4 hr and placed into culture dishes containing a feeder layer of glia isolated 2 weeks prior from postnatal day 1 rat cortex. The growth medium was defined, containing N2-supplemented MEM. Cultures were maintained by feeding with growth media twice weekly.

Construction and Purification of Fusion Proteins

H_6KA2(c-term) was prepared by subcloning the EcoRI fragment into pTrcHisB (Invitrogen). This fragment begins just past the predicted transmembrane 4 domain and contains the entire predicted C terminus (amino acids 804–961) and approximately 500 nucleotides of 3′-untranslated sequence. H_6KA2(c-term) contains an N-terminal hexahistidine tag followed by a T7 epitope engineered into the vector. In all, there is a 33 amino acid linker present between the histidine tag and the beginning of the KA2 sequence of interest. Synthesis of recombinant proteins in TOP10 cells (Invitrogen) was induced by 1 mM isopropyl-β-D-thiogalactopyranoside for 12–14 hr at 37°C. Cells were then harvested, lysed by French Press as directed by the manufacturer (SLM Instruments, Inc.) and centrifuged at 70,000 × g for 25 min at 4°C. The pellet was solubilized in 8 M urea with mixing for 1 hr at room temperature, and centrifuged at 70,000 × g for 25 min at room temperature. Solubilized H_6KA2(c-term) was bound to Ni^{+2}/NTA beads (Qiagen) for 1 hr at room temperature with mixing and then loaded into a column. H_6KA2(c-term) was renatured using a 6 M - 1 M urea gradient prepared in 500 mM NaCl, 50 mM sodium phosphate (pH 7.5), 10 mM Tris (pH 7.5), and 20% glycerol over the course of 2 hr. Renatured H_6KA2(c-term) was eluted from the Ni^{+2}/NTA beads using an imidazole step gradient from 50 to 500 mM in PBS, then dialyzed to remove the imidazole.

To construct H_6rbSec1A, the entire coding sequence of rbSec1A (Garcia et al., 1996) was subcloned into pTrcHisB at the EcoRI site. Recombinant H_6rbSec1A protein was induced in TOP10 cells and purified on Ni^{+2}/NTA beads (Qiagen) according to the manufacturer's instructions. GST-fusion proteins with specific regions of SAP90 and SAP90W470A were constructed by subcloning PCR-amplified DNA fragments directionally into the EcoRI-SalI sites of pGEX-4T (Pharmacia). Vectors expressing GST-SAP90 fusion proteins contain the SAP cDNA sequence encoding the following amino acids: GST-PDZ1 (2–151), GST-PDZ2 (156–266), GST-PDZ3 (300–401), GST-PDZ1+2 (2–266), GST-PDZ2+3 (156–401), GST-SH3 (402–500), and GST-GK (521–724). To generate the GluR6(c-term), B-UP, B-DN, B-UPmt, and B-DNmt cDNAs, synthetic DNA sequences encoding the 15 C-terminal amino acids (894–908) of GluR6 or nucleotide sequences encoding the peptide sequences as shown in Figure 3D, respectively, were ligated in frame with a biotinylation signal sequence into the HindIII and BglII restriction sites of the PinPoint Xa-3 vector (Promega). Constructs were verified by nucleotide sequencing. Recombinant proteins were prepared and purified according to the manufacturer's instructions except for GST-SH3; in this case, induction was performed at 30°C to minimize degradation. Protein concentrations were determined with the Bio-Rad protein assay.

Affinity Chromatography

Fifty micrograms of H_6KA2(c-term) or H_6rbSec1A was prebound to Ni^{+2}/NTA sepharose beads in PBS/1% Triton X-100/40 mM imidazole for 1 hr at 4°C, washed to remove unbound protein, and incubated with 1 mg of protein extract overnight at 4°C with continuous mixing and washed three times. Recombinant protein and any associated proteins were eluted from the Ni^{+2}/NTA sepharose beads using a step gradient of 50, 100, 250, and 500 mM imidazole. Recombinant protein elution peaked at 250 mM imidazole as determined by Coomassie blue staining of eluates separated by SDS-PAGE. One-tenth of the peak fraction was separated by SDS-PAGE, transferred to nitrocellulose, and immunoblotted as described below. In the case of GST fusion proteins, modifications were as follows: GST fusion proteins (10 μg) were prebound to glutathione sepharose 4B beads in RIPA (1% NP-40, 0.5% sodium deoxycholate, 100 μg/ml PMSF, 10 μg/ml aprotinin, 10 μg/ml leupeptin, and 10 μg/ml pepstatin A in PBS) for 1 hr at 4°C and washed. Twenty micrograms of the binding partner was added in RIPA buffer and incubated overnight with mixing. After extensive washes in RIPA/300–500 mM NaCl/40 mM imidazole, elutions were performed in 10 mM glutathione/50 mM Tris (pH 8.0). Eluates were analyzed by SDS-PAGE, Western blotted, and visualized by chemiluminesence as directed by the manufacturer (Amersham).

Protein Preparation, Immunoblotting, and Immunoprecipitation

For affinity chromatography experiments, frozen adult rat brains (Pel-Freeze) were homogenized in PBS with protease inhibitors (100 μg/ml PMSF, 10 μg/ml aprotinin, 10 μg/ml leupeptin, and 10μg/ml pepstatin A) using a Tissuemizer (Tekmar) and centrifuged at 4°C at 800 × g. Triton X-100 was added to the resulting supernatant to a final concentration of 1%. Proteins were solubilized for 1 hr at 4°C and clarified by centrifugation at 165,000 × g for 1 hr. Cell culture protein extracts were similarly prepared with the following modification. Forty-eight hours after transfection, cells were removed from tissue culture flasks using 2 mM EDTA (pH 8.0) in PBS, washed, and pelleted. Pelleted cells were then solubilized as described above.

For immunoprecipitation (IP) experiments, fresh adult rat brains were homogenized as above and centrifuged at 4°C for 1 hr at 165,000 × g. Insoluble pellets were dissolved in RIPA with 2% SDS. Solublized extracts were passaged several times through a 25-gauge needle, diluted to a final SDS concentration of 0.33%, and centrifuged at 10,000 × g for 5 min. Transfected cell extracts were prepared in a similar fashion, except 0.2% SDS was used in the solubilization. Immunoprecipitations were performed by incubating

extracts with 2 μg of anti-GluR1 (gift of Dr. R. Huganir), or anti-GluR6, -NR2A, or -KA2 (Upstate Biotechnology) antibodies for 2 hr at 4°C, followed by incubation with 100 μl of protein G-Sepharose (Pharmacia) for 12–16 hr and four washes in RIPA buffer. Western blot analysis of the depleted cell extracts showed no detectable anti-GluR6 or anti-KA2 immunoreactivity, suggesting that immunoprecipitation was complete. Bound proteins were eluted from the beads by boiling and then separated by SDS-PAGE. As controls, rat brain extract or crude whole-cell extracts of transfected cells were used; for these lanes (lane 1 in Figure 2A; lanes 1–3 in Figure 2B), 5 μg of protein was loaded (1% of the amount of immunoprecipitated proteins loaded in the other lanes). Gels were then Western blotted and immunostained as previously described (Garcia et al., 1996). Scanning densitometry of the amounts of SAP90 coimmunoprecipitated in Figure 2A indicates that anti-NR2A immunoreactivity was 75% (lane 4), anti-GluR6 was 84% (lane 6), and anti-KA2 (lane 8) was 25% of the SAP90 immunoreactivity detected in rat brain extract (lane 1). Primary antibodies used were as follows: mouse monoclonal anti-SAP90 (Transduction Labs, 1:250), mouse monoclonal anti-SAP97 (1:2000), rabbit polyclonal anti-SAP102 (1:2000), and mouse monoclonal anti-T7 antibody (Novagen, 1:10,000).

ELISA

ELISA was performed as described (Müller et al., 1996) with slight modifications. MaxiSorp 96-well immunoplates (Nunc) were incubated overnight at 4°C with 50 μl of H_6KA2(c-term) or NR2B C terminus at the concentration of 1.6 μg/ml in 125 mM borate, 75 mM NaCl (BBS [pH 8.5]). After four washes with BBS, plates were incubated with 1% bovine serum albumin (BSA) for 2 hr at room temperature. Plates were washed four times with BBS, and 50 μl of 2-fold serial dilutions of GST-fusion proteins was added to four rows. After overnight incubation at 4°C, plates were washed four times with BBS, incubated with rabbit anti-GST polyclonal antibody (Sigma; 1:1000 in 1% BSA in BBS) for 2 hr at 4°C, washed four times with BBS, and incubated with anti-rabbit alkaline phosphatase antibody (Sigma; 1:1000 in 1% BSA in BBS) for 2 hr at 4°C. Plates were then washed four times with BBS, and the color reaction performed at room temperature using 200 μl of 1 mg/ml of p-nitrophenyl phosphate in reaction buffer (0.1 mM $MgCl_2$, 5% v/v diethanolamine [pH 9.8]). Enzymatic reaction was stopped by adding 50 μl of 3N NaOH to each well. Microtiter plates were read at 410 nm using a Dynatech plate reader. Origin 4.1 was used to fit data in the Hill equation ($Abs = Abs_{max}/1+[EC50/[X]]^n$; Abs = absorbance at 410 nm) using a nonlinear least-squares algorithm.

Immunocytochemistry

Forty-eight hours after transfection, COS-1 and HEK293 cells were fixed for 20 min on ice in 2% paraformaldehyde in PBS and, except when utilizing antibodies against extracellular epitopes, permeabilized in 0.1% Triton X-100 for 20 min at room temperature. Staining was visualized by indirect immunofluorescence. Cells were incubated with a mouse monoclonal anti-c-myc (Santa Cruz, 1:100 dilution) or IgM mouse monoclonal anti-GluR5, 6 and 7 (Pharmingen, 1:200 dilution), or rabbit polyclonal anti-KA2 (Upstate Biotechnology, 10 μg/ml) primary antibodies for 2 hr at room temperature, using 4% goat serum (Gemini Bio-Products) to block nonspecific sites. After four washes with PBS/0.05% Tween-20, cells then were stained with anti-mouse IgG-FITC (Becton Dickinson 1:200), anti-rabbit-Cy3 (Jackson Immunoresearch 1:200), or anti-mouse IgM-Cy3 (Jackson ImmunoResearch Lab, 1:500) secondary antibodies and washed four times. For double labeling of GluR6 and SAP90, cells were first labeled with anti-GluR6, washed, then permeabilized and stained with anti-SAP90 antibodies (Transduction Labs, 1:250). After washing, cells were incubated with Cy3-conjugated anti-mouse IgM antiserum, washed, and finally stained with anti-mouse IgG-FITC. Coverslips were mounted on glass slides in 90% glycerol in PBS and fluorescence visualized using Zeiss Axiovert 100 laser scanning confocal microscope. Controls for staining of intracellular epitopes (anti-KA2, anti-C-terminal GluR6, and anti-c-myc [c-myc-tagged SAP90] antibodies) were performed under the same conditions but without permeabilizaition; no staining was observed.

Cultured hippocampal neurons were fixed with 4% paraformaldehyde for 10 min at 37°C, washed in HEPES-buffered MEM (MEMH; GIBCO), permeabilized for 5 min with 0.05% saponin in MEMH supplemented with 10% horse serum plus 1% goat serum, and then incubated with a mouse monoclonal anti-SAP102 (1:250), a mouse monoclonal anti-SAP90 (Transduction Labs, 1:250), and a rabbit polyclonal anti-KA2 or anti-GluR6 (Upstate Biotechnology, 10 μg/ml) primary antibody overnight at 4°C. Labeling was again visualized by indirect immunofluorescence. For rabbit polyclonal primary antibodies, cells were subsequently exposed to CY3-conjugated anti-rabbit antibodies. When the primary antibody was monoclonal, cells were sequentially incubated in biotin-conjugated anti-mouse secondary antibodies and FITC-conjugated streptavidin. Stained coverslips were mounted in Citifluor and labeling visualized under fluorescence optics with a Nikon Eclipse E800 microscope.

Electrophysiology

Patch-clamp recordings were performed on transiently transfected cells 2 to 4 days after transfection using the permeabilized-patch variation of standard whole-cell patch recording procedures (Rae et al., 1991). A List EPC-9 patch clamp amplifier was employed in conjunction with MacIntosh-based data acquisition and analysis software (HEKA, Instrutech Corp.). Analog signals were low-pass filtered at 10 kHz (-3dB, digital Gaussian filter) and stored on videotape using a VR10 digital data interface (Instrutech) and a VCR at a sampling rate of 94 kHz. For kinetic analysis, the HEKA software was used to digitize the stored analog data (sample interval, 20 μs; low-pass filter, 5 kHz) and to analyze exponential decay rates, which were fitted using a Simplex least-squares algorithm.

Patch pipettes were constructed from Corning 8161 glass capillary tubing (Warner Instruments) and had initial resistances of 3 to 4 MΩ when filled with the internal recording solution. The pipette solution (pH 7.2) contained (in mM): CsCl, 150; $CaCl_2$, 0.5; Na-EGTA, 5; and K-HEPES, 10, as well as amphotericin B (final concentration, 0.25 mg/ml) to permeabilize the patch and allow low-resistance electrical access without breaking the patch membrane. The normal extracellular solution (pH 7.2) contained (in mM): NaCl, 150; KCl, 2.5; $CaCl_2$, 1; Na-HEPES, 10. Rapid perfusion of receptor ligands, dissolved in extracellular saline, was carried out using a rapid superfusion system (ALA Scientific Instruments). This system utilizes solenoid valves to regulate solution flow through fine bore capillary tubing (100 μm ID) connected to a micromanifold; four solutions (one of extracellular saline without ligand plus three containing ligand) could be held simultaneously. Each solution is under pressure (~6 lb/in^2), so that when a valve is opened the solution will rapidly perfuse the cell; "dead space" <1 μl (ALA Scientific Instruments). Potential movement artifacts were assessed by perfusion of the normal extracellular saline (without ligand). All recordings were performed at room temperature (20°C–22°C).

Acknowledgments

We thank Dr. Morgan Sheng for the PSD-95 (SAP90) and chapsyn 110 clones; Drs. Jim Boulter and Steve Heinemann for all the glutamate receptor clones used in this study; Dr. Ed Hawrot for Trx-αT68-H_6 and H_6-αBgTx histidine-tagged recombinant proteins; and Dr. Rick Huganir for KA2 and GluR6 blocking peptides. We also thank Jeremy Edgerton who helped with some of the plasmid constructs and confocal microscopy, Dinesh Bahl who made the GluR6(Q) construct, and Kendra Bence and Ryuzo Shingai for helpful comments. This research was supported by R29 NS 33914-02 (National Institutes of Health) and SA047 (Council for Tobacco Research Scholar Award) to J. M.

Received December 18, 1997; revised July 28, 1998.

References

Bartlett, W.P., and Banker, G.A. (1984). An electron microscopic study of the development of axons and dendrites of hippocampal neurons in culture: II. synaptic relationships. J. Neurosci. *4*, 1954–1965.

Bettler, B., Boulter, J., Hermans-Borgmeyer, I., O'Shea-Greenfield, A., Deneris, E.S., Moll, C., Borgmeyer, U., Hollmann, M., and Heinemann, S.F. (1990). Cloning of a novel glutamate receptor subunit,

GluR5: expression in the nervous system during development. Neuron *5*, 583–595.

Brenman, J.E., Chao, D.S., Gee, S.H., McGee, A.W., Craven, S.E., Santillano, D.R., Wu, Z., Huang, F., Xia, H., Peters, M.F., Froehner, S.C., and Bredt, D.S. (1996). Interaction of nitric oxide synthase with the postsynaptic density protein PSD-95 and α1-syntrophin mediated by PDZ domains. Cell *84*, 757–767.

Bunnel, S.C., Henry, P.A., Kolluri, R., Kirchhausen, T., Rickles, R.J., and Berg, L.J. (1997). Identification of Itk/Tsk Src homology 3 domain ligands. J. Biol. Chem. *271*, 25646–25656.

Castillo, P.E., Malenka, R.C., and Nicoll, R.A. (1997). Kainate receptors mediate a slow postsynaptic current in hippocampal CA3 neurons. Nature *388*, 182–186.

Chen, C., and Okayama, H. (1987). High efficiency transformation of mammalian cells by plasmid DNA. Mol. Cell. Biol. *7*, 2745–2752.

Cho, K.O., Hunt, C.A., and Kennedy, M.B. (1992). The rat brain postsynaptic density fraction contains a homolog of the Drosophila discs-large tumor suppressor protein. Neuron *9*, 929–942.

Clarke, V.R.J., Ballyk, B.A., Hoo, K.H., Mandelzys, A., Pellizzari, A., Bath, C.P., Thomas, J., Sharpe, E.F., Davies, C.H., Ornstein, P.L., et al. (1997). A hippocampal GluR5 kainate receptor regulating inhibitory synaptic transmission. Nature *389*, 599–603.

Cohen, N.A., Brenman, J.E., Snyder, S.H., and Bredt, D.S. (1996). Binding of the inward rectifier K^+ channel Kir 2.3 to PSD-95 is regulated by protein kinase A phosphorylation. Neuron *17*, 759–767.

Craig, A.M., Blackstone, C.D., Huganir, R.L., and Banker, G. (1993). The distribution of glutamate receptors in cultured rat hippocampal neurons: postsynaptic clustering of AMPA-selective subunits. Neuron *10*, 1055–1068.

Dawson, T.M., Dawson, V.L., and Snyder, S.H. (1992). A novel neuronal mesenger molecule in brain: free radical, nitric oxide. Ann. Neurol. *32*, 297–311.

Doyle, D.A., Lee, A., Lewis, J., Kim, E., Sheng, M., and MacKinnon, R. (1996). Crystal structures of a complexed and peptide-free membrane protein-binding domain: molecular basis of peptide recognition by PDZ. Cell *85*, 1067–1076.

Egebjerg, J., Bettler, B., Hermans-Borgmeyer, I., and Heinemann, S.F. (1991). Cloning of a cDNA for a glutamate receptor subunit activated by kainate but not AMPA. Nature *351*, 745–748.

Ehlers, M.D., Mammen, A.L., Lau, L.F., and Huganir, R.L. (1996a). Synaptic targeting of glutamate receptors. Curr. Opin. Cell. Biol. *8*, 484–489.

Ehlers, M.D., Shang, S., Bernhardt, J.P., and Huganir, R.L. (1996b). Inactivation of NMDA receptors by direct interaction of calmodulin with the NR1 subunit. Cell *84*, 745–755.

Erpel, T., Superti-Furga, G., and Courtneidge, S.A. (1995). Mutational analysis of the Src SH3 domain: the same residues of the ligand binding surface are important for intra- and intermolecular interactions. EMBO. J. *14*, 963–975.

Feng, S., Kasahara, C., Rickles, R.J., and Schreiber, S.L. (1995). Specific interactions outside the proline-rich core of two classes of Src homology 3 ligands. Proc. Natl. Acad. Sci. USA *92*, 12408–12415.

Garcia, E.P., McPherson, P.S., Chilcote, T.J., Takei, K., and De Camilli, P. (1996). rbSec1A and B colocalize with syntaxin 1 and SNAP-25 throughout the axon, but are not in a stable complex with syntaxin. J. Cell. Biol. *129*, 105–120.

Goslin, K., and Banker, G. (1991). Rat hippocampal neurons in low density. In Culturing Nerve Cells, G. Banker and K. Goslin, eds. (Cambridge, MA: MIT Press), pp. 251–282.

Harris, E.W., and Cotman, C.W. (1986). Long-term potentiation of guinea-pig mossy fibre responses is not blocked by N-methyl-D-aspartate antagonists. Neurosci. Lett. *70*, 132–137.

Herb, A., Burnashev, N., Werner, P., Sakmann, B., Wisden, W., and Seeburg, P.H. (1992). The KA-2 subunit of excitatory amino acid receptors shows widespread expression in brain and forms ion channels with distantly related subunits. Neuron *8*, 775–785.

Hollmann, M., and Heinemann, S.F. (1994). Cloned glutamate receptors. Annu. Rev. Neurosci. *17*, 31–108.

Huettner, J.E. (1990). Glutamate receptor channels in rat DRG neurons: activation by kainate and quisqualate and blockade of desensitization by Con A. Neuron *5*, 255–266.

Hunt, C.A., Schenker, L.J., and Kennedy, M.B. (1996). PSD-95 is associated with the postsynaptic density and not with the presynaptic membrane at forebrain synapses. J. Neurosci. *16*, 1380–1388.

Huntley, G.W., Rogers, S.W., Moran, T., Janssen, W., Archin, N., Vickers, J.C., Cauley, K., Heinemann, S.F., and Morrison, J.H. (1993). Selective distribution of kainate receptors subunits immunoreactivity in monkey neocortex revealed by a monoclonal antibody that recognizes glutamate receptor subunits GluR5/6/7. J. Neurosci. *13*, 2965–2981.

Jones, M.V., and Westbrook, G.L. (1996). The impact of receptor desensitization on fast synaptic transmission. Trends Neurosci. *19*, 96–101.

Kennedy, M.B. (1997). The postsynaptic density at glutamatergic synapses. Trends Neurosci. *20*, 264–268.

Kim, E., and Sheng, M. (1996). Differential K^+ channel clustering activity of PSD-95 and SAP97, two related membrane-associated putative guanylate kinases. Neuropharmacol. *35*, 993–1000.

Kim, E., Niethammer, M., Rothschild, A., Jan, Y.N., and Sheng, M. (1995). Clustering of Shaker-type K^+ channels by interaction with a family of membrane-associated guanylate kinases. Nature *378*, 85–86.

Kim, E., Cho, K.O., Rothschild, A., and Sheng, M. (1996). Heteromultimerization and NMDA receptor-clustering activity of Chapsyn-110, a member of the PSD-95 family of proteins. Neuron *17*, 103–113.

Kim, E., Naisbitt, S., Hsueh, Y.P., Rao, A., Rothschild, A., Craig, A.M., and Sheng, M. (1997). GKAP, a novel synaptic protein that interacts with the guanylate kinase-like domain of the PSD-95/SAP90 family of channel clustering molecules. J. Cell. Biol. *136*, 669–678.

Kim, J.H., Liao, D., Lau, L.-F., and Huganir, R.L. (1998). SynGAP: a synaptic RasGAP that associates with the PSD-95/SAP90 protein family. Neuron *20*, 683–691.

Kirsch, J., and Betz, H. (1998). Glycine-receptor activation is required for receptor clustering in spinal neurons. Nature *392*, 717–720.

Kistner, U., Wenzel, B.M., Veh, R.W., Cases-Langhoff, C., Garner, A., Appeltauer, U., Voss, B., Gundelfinger, E.D., and Garner, C.C. (1993). SAP90, a rat presynaptic protein related to the product of the Drosophila tumor suppressor gene dlg-A. J. Biol. Chem. *268*, 4580–4583.

Kornau, H.C., Schenker, L.T., Kennedy, M.B., and Seeburg, P.H. (1995). Domain interaction between NMDA receptor subunits and the postsynaptic density protein PSD-95. Science *269*, 1737–1740.

Kuhlendahl, S., Spangenberg, O., Konrad, M., Kim, E., and Garner, C.C. (1998). Functional analysis of the guanylate kinase-like domain in the synapse-associated protein SAP97. Eur. J. Biochem., in press.

Lahey, T., Gorczyca, M., Jia, X.X., and Budnik, V. (1994). The Drosophila tumor suppressor gene *dlg* is required for normal synaptic bouton structure. Neuron *13*, 823–835.

Lee, C.H., Leung, B., Lemmon, M.A., Zheng, J., Cowburn, D., Kuriyan, J., and Saksela, K. (1995). A single amino acid in the SH3 domain of Hck determines its high affinity and specificity in binding to HIV-1 Nef protein. EMBO J. *14*, 5006–5015.

Lerma, J. (1997). Kainate reveals its targets. Neuron *19*, 1155–1158.

Lerma, J., Paternain, A.V., Naranjo, J.R., and Mellstrom, B. (1993). Functional kainate-selective glutamate receptor in cultured hippocampal neurons. Proc. Natl. Acad. Sci. USA *90*, 11688–11692.

Marshall, J., Molloy, R., Moss, G.W.J., Howe, J.R., and Hughes, T.E. (1995). The jellyfish green fluorescent protein: a new tool for studying ion channel expression and function. Neuron *14*, 211–215.

Matoskova, B., Wong, W.T., Nomura, N., Robbins, K.C., and Di Fiore, P.P. (1996). RN-tre specifically binds to the SH3 domain of eps8 with high affinity and confers growth advantage to NIH3T3 upon carboxy-terminal truncation. Oncogene *12*, 2679–2688.

Mayer, B.J., and Eck, M.J. (1995). SH3 domains: minding your p's and q's. Curr. Biol. *5*, 364–367.

McPherson, P., Garcia, E.P., David, C., Takei, K., and DeCamilli, P. (1996). A presynaptic inositol-5-phosphatase. Nature *379*, 353–357.

Mulle, C., Sailer, A., Pèrez-Otaño, I., Dickinson-Anson, H., Castillo, P.E., Bureau, I., Maron, C., Gage, F.H., Mann, J.R., Bettler, B., and

Heinemann, S.F. (1998). Altered synaptic physiology and reduced susceptibility to kainate-induced seizures in GluR6-deficient mice. Nature *392*, 601–605.

Müller, B.M., Kistner, U., Veh, R.W., Cases-Langhoff, C., Becker, B., Gundelfinger, E.D., and Garner, C.C. (1995). Molecular characterization and spatial distribution of SAP97, a novel presynaptic protein homologous to SAP90 and the Drosophila Discs-Large Tumor Suppressor protein. J. Neurosci. *15*, 2354–2366.

Müller, B.M., Kistner, U., Kindler, S., Chung, W.J., Kuhlendahl, S., Fenster, S.D., Lau, L.F., Veh, R.W., Huganir, R.L., Gundelfinger, E.D., and Garner, C.C. (1996). SAP102, a novel postsynaptic protein that interacts with NMDA receptor complexes in vivo. Neuron *17*, 255–265.

Naisbitt, S., Kim, E., Weinberg, R.J., Rao, A., Yang, F.C., Craig, A.M., and Sheng, M. (1997). Characterization of guanylate kinase-associated protein, a postsynaptic density protein at excitatory synapses that interacts directly with postsynaptic density-95/synapse-associated protein 90. J. Neurosci. *17*, 5687–5696.

Niethammer, M., Kim, E., and Sheng, M. (1996). Interaction between the C terminus of NMDA receptor subunits and multiple members of the PSD-95 family of membrane-associated guanylate kinases. J. Neurosci. *16*, 2157–2163.

Niethammer, M., Valtschanoff, J.G., Kapoor, T.M., Allison, D.W., Weinberg, R.J., Craig, A.M., and Sheng, M. (1998). CRIPT, a novel postsynaptic protein that binds to the third PDZ domain of PSD-95/SAP90. Neuron *20*, 693–707.

Otis, T., Zhang, S., and Trussell, L.O. (1996). Direct measurement of AMPA receptor desensitization induced by glutamatergic synaptic transmission. J. Neurosci. *16*, 7496–7504.

Paternain, A.V., Morales, M., and Lerma, J. (1995). Selective antagonism of AMPA receptors unmasks kainate receptor-mediated responses in hippocampal neurons. Neuron *14*, 185–189.

Pawson, T., and Scott, J.D. (1997). Signaling through scaffold, anchoring, and adaptor proteins. Science *278*, 2975–2080.

Rae, J., Cooper, K., Gates, P., and Watsky, M. (1991). Low access resistance perforated patch recordings using amphotericin B. J. Neurosci. Meth. *37*, 15–26.

Rao, A., Kim, E., Sheng, M., and Craig, A.M. (1998). Heterogeneity in the molecular composition of excitatory postsynaptic sites during development of hippocampal neurons in culture. J. Neurosci. *18*, 1217–1229.

Raymond, L.A., Blackstone, C.D., and Huganir, R.L. (1993). Phosphorylation and modulation of recombinant GluR6 glutamate receptors by cAMP-dependent protein kinase. Nature *361*, 637–641.

Sastry, L., Lin, W., Wong, W.T., Di Fiore, P.P., Scoppa, C.A., and King, C.R. (1995). Quantitative analysis of Grb2-Sos1 interaction: the N terminal SH3 domain of Grb2 mediates affinity. Oncogene *11*, 1107–1112.

Schiffer, H.H., Swanson, G.T., and Heinemann, S.F. (1997). Rat GluR7 and a carboxy-terminal splice variant, GluR7b, are functional kainate receptor subunits with a low sensitivity to glutamate. Neuron *19*, 1141–1146.

Seeburg, P.H. (1993). The molecular biology of mammalian glutamate receptor channels. Trends Neurosci. *16*, 359–648.

Sheng, M. (1996). PDZs and receptor/channel clustering: rounding up the latest suspects. Neuron *17*, 575–578.

Shieh, B-H., and Zhu, M.-Y. (1996). Regulation of the TRP Ca^{2+} channel by InaD in Drosophila photoreceptors. Neuron *16*, 991–998.

Swanson, G.T., Gereau, R.W., Green, T., and Heinemann, S.F. (1997). Identification of amino acid residues that control functional behavior in GluR5 and GluR6 kainate receptors. Neuron *19*, 913–926.

Tsunoda, S., Sierralta, J., Sun, Y., Bodner, R., Suzuki, E., Becker, A., Socolich, M., and Zucker, C.S. (1997). A multivalent PDZ-domain protein assembles signaling complexes in a G-protein-coupled cascade. Nature *288*, 243–249.

Vignes, M., and Collingridge, G.L. (1997). The synaptic activation of kainate receptors. Nature *388*, 179–182.

Wang, L.-Y., Taverna, F.A., Huang, X.-P., MacDonald, J.F., and Hampson, D.R. (1993). Phosphorylation and modulation of a kainate receptor (GluR6) by cAMP-dependent protein kinase. Science *259*, 1173–1175.

Weng, Z., Rickles, R.J., Feng, S., Richard, S., Shaw, A.S., Schreiber, S.L., and Brugge, J.S. (1995). Structure-function analysis of SH3 domains: SH3 binding specificity altered by single amino acid substitutions. Mol. Cell. Biol. *15*, 5627–5634.

Wenthold, R.J., Trunpy, V.A., Zhu, W.-S., and Petralia, R.S. (1994). Biochemical and assembly properties of GluR6 and KA2, two members of the kainate receptor family, determined with subunit-specific antibodies. J. Biol. Chem. *269*, 1332–1339.

Wilding, T.J., and Huettner, J.E. (1997). Activation and desentization of hippocampal kainate receptors. J. Neurosci. *17*, 2713–2721.

Woods, D.F., and Bryant, P.J. (1991). The discs-large tumor suppressor gene of Drosophila encodes a guanylate kinase homolog localized at septate junctions. Cell *66*, 451–464.

Wyszynski, M., Lin, J., Rao, A., Nigh, E., Beggs, A.H., Craig, A.M., and Sheng, M. (1997). Competitive binding of alpha-actinin and calmodulin to the NMDA receptor. Nature *385*, 439–442.

Zorumski, C.F., Mennerick, S., and Que, J. (1996). Modulation of excitatory synaptic transmission by low concentrations of glutamate in cultured rat hippocampal neurons. J. Physiol. *494*, 465–477.